

# Color Gamut Characterization via Ray Tracing for Device Profile Generation

*Dmitri A. Gusev*  
*NexPress Solutions LLC*  
*Rochester, New York*

## Abstract

Color gamut characterization is an essential step in the ICC profile generation for imaging devices. It is also needed as part of evaluation and comparison of image quality achievable by different imaging systems. A novel technique is presented for characterizing the color gamut of an imaging device via ray tracing in the CIELAB color space. Initially, the convex hull of the set of measurement points is computed in the device space. Each of the resulting simplices in the convex hull structure has a set of CIELAB data triples associated with its vertices. The "local" convex hull is computed for each of those sets separately in CIELAB. The convex hull triangles are then subjected to a ray tracing procedure aimed at approximating the maximum achievable chroma for a set of pairs of L and hue angle values. For the purpose of the device profile generation, this set is derived from the set of grid points in the PCS (profile connection space) that have to be mapped to the device space. It is shown that the new method characterizes the gamut surface and volume better than the conventional technique based on computing the "global" convex hull of the measurement data points in CIELAB.

## 1. Introduction

A *color gamut* is a region in a color space, containing colors reproducible by a given imaging device or present in a given image. Color gamut characterization is an essential part of *device characterization*, a process that determines the rules of color reproduction by a given device. In particular, it is needed as a step of the ICC profile generation. (For the details on device characterization by means of the ICC color profiles, we refer the reader to Ref. [1].) Color gamut characterization is also useful for evaluation and comparison of image quality achievable by different imaging systems, gamut visualization, and gamut volume calculation.

For the digital imaging devices that specify the amounts of colorants to be combined in a given pixel in terms of discrete values (say, integers) from finite ranges, the notions of the gamut boundary and gamut volume are merely useful abstractions, as the actual gamuts have gaps that are ignored. Furthermore, for an analog imaging

device with a solid-volume gamut, an infinite number of color patch measurements would be needed in order to reconstruct the gamut boundary exactly. Approaches to approximate reconstruction of the gamut boundary are divided into two groups<sup>2</sup>: (a) *geometric methods*, which are based solely on a set of point coordinates in a device-independent color space, such as CIELAB,<sup>3</sup> and (b) *colorant space methods*, which use the device color space information as well.

The most popular geometric method for color gamut characterization is based on computation of a 3D "global" *convex hull* of the in-gamut data points in CIELAB.<sup>4</sup> (The convex hull of a set of points is the smallest convex set that contains the points.) For the real imaging systems, this method tends to overestimate the gamut volume, because the realistic color gamuts are non-convex. As the number of sufficiently uniformly distributed in-gamut data points increases, convergence to the "true" value corresponding to our notion of color gamut is not guaranteed. The information on implementation of the convex hull algorithms can be found in Ref. [5]. An attempt to improve the convex hull method was made by Balasubramanian and Dalal.<sup>6</sup> For brevity, we will call their modification "*concave*" hull. It involves artificial "inflation" of the data set before computing its convex hull. As a result, interior points may be incorrectly identified as surface points, in which case the gamut volume will be underestimated after the appropriate "deflation". Cholewo and Love<sup>2</sup> introduced a more complicated geometric method based on the concept of *alpha-shapes*, mathematical generalizations of the convex hull. The resulting gamut shape and volume depend on the value of a special parameter  $\alpha$  that the authors of the method recommended to determine experimentally for each given imaging system. The deficiencies of the geometric methods are due primarily to their fundamental lack of the device space information. Their primary advantage is the ability to handle the task for the systems, for which the device space data is unavailable. However, this advantage loses its value if there is a need to complete the device characterization afterwards.

The colorant space methods assume that each surface point in the device-independent color space can be achieved by combining the colorants so that at least one of the device space coordinates attains its minimum or maximum value. This is a reasonable assumption for the

printing processes that utilize three or more colorants. Indeed, for any given point inside the device space gamut, we are very likely to find three colorants such that (a) addition of a sufficiently small amount of any of these colorants does not bring us to the same point in the device-independent space as subtraction of another small amount of that same colorant, and (b) the vectors tangential to the corresponding trajectories in the device-independent space form a basis in it, so there exists a radius so small that any point within this radius from the location of the given point in the device-independent space can be reproduced by adjusting the amounts of these colorants appropriately. However, as we have already pointed out, an actual imaging device may be unable to control the amounts of colorants with arbitrary precision, so the given point is not 100% guaranteed to map to an interior point in the device-independent space. Braun and Fairchild<sup>7</sup> considered the limited case of three colorants and stated that, if the gamut data were represented as a 3D wire-frame mesh in CIELAB space, some type of estimation process would be required to extract a slice profile of the gamut surface for a given *hue angle*

$$h = \arctan(b/a). \quad (1)$$

(In this paper, the letters 'L', 'a', and 'b' denote the CIELAB coordinates also known as  $L^*$  (*lightness*),  $a^*$ , and  $b^{*3,7}$ ) Braun and Fairchild further suggested that this estimation process might involve a series of ray tracing steps where the gamut intersection points would be located for a series of L values for the given hue angle. They did not actually implement the ray tracing approach. Instead, they preferred to project the data on the Lh plane. They subsequently looked up or interpolated values from the resulting 2D matrix. In the past, when there were more than three colorants involved, the gamuts of the three-colorant subprocesses were computed and then their union was taken to be the gamut of the process of interest.<sup>8</sup> The problem with this approach is that some surface points can only be achieved by applying more than three colorants simultaneously.

In the next section of this paper, a new, general colorant space method for color gamut characterization via ray tracing is presented. Section 3 will describe application of the ray tracing method to device profile generation.

## 2. Gamut Characterization via Ray Tracing

Let  $N$  be the dimensionality of the imaging device space,  $N \geq 3$ . The convex hull of a set of measurement points in this space consists of  $(N-1)$ -simplices,  $N$  vertices per simplex. Each of these vertices has a CIELAB data triple associated with it. For each  $(N-1)$ -simplex, we take the set of data triples associated with its vertices and compute the "local" convex hull in CIELAB. CIELAB is a 3D color space, so the elements of the local convex hull structures are triangles. One of these triangles is shown in Figure 1. It is defined by three data points in CIELAB:  $(L_1, a_1, b_1)$ ,  $(L_2, a_2, b_2)$ , and  $(L_3, a_3, b_3)$ . For the purpose of color gamut

characterization, all such triangles with positive areas will be subjected to a ray tracing procedure as follows.

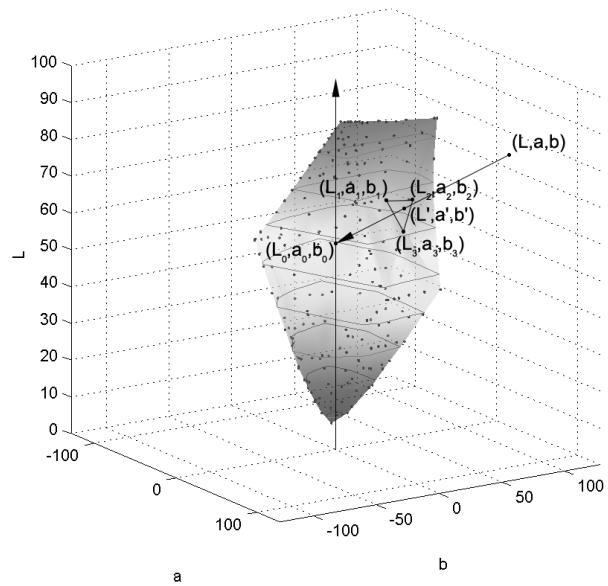


Figure 1. Ray tracing in CIELAB

First, a set of  $(L, h)$ -pairs is chosen so that the value ranges of  $L$  and  $h$  are sampled sufficiently well. For example, we may look at all combinations of  $L=0, 1, \dots, 100$  and  $h=0^\circ 30', 1^\circ 30', \dots, 359^\circ 30'$ . For each value of  $h$ , the values of  $a$  and  $b$  are computed so that Eq. (1) is true. The resulting CIELAB point  $(L, a, b)$  for one of the  $(L, h)$ -pairs is shown in Fig. 1.

Let the symbol 'T' denote *transposition* and consider three vectors  $\mathbf{x}_1$ ,  $\mathbf{x}_2$  and  $\mathbf{x}_3$  defined by the equation

$$\mathbf{x}_i = [L_i \ a_i \ b_i]^T, \quad (2)$$

where  $i=1, 2, 3$ . The *vector product* (*cross-product*) of the vector differences  $(\mathbf{x}_3 - \mathbf{x}_2)$  and  $(\mathbf{x}_1 - \mathbf{x}_2)$ ,

$$\mathbf{n} = (\mathbf{x}_3 - \mathbf{x}_2) \times (\mathbf{x}_1 - \mathbf{x}_2), \quad (3)$$

is the *normal* to the plane  $P$  defined by  $(L_1, a_1, b_1)$ ,  $(L_2, a_2, b_2)$ , and  $(L_3, a_3, b_3)$ .

For any point  $(L_0, a_0, b_0)$  not coinciding with the point  $(L, a, b)$ , we can find all points of intersection of  $P$  and the straight line  $R$  that connects  $(L_0, a_0, b_0)$  and  $(L, a, b)$ . In order to achieve that, we define the vector

$$\mathbf{v} = [L - L_0 \ a - a_0 \ b - b_0]^T. \quad (4)$$

and observe that if the *scalar product*  $\langle \mathbf{n}, \mathbf{v} \rangle$  is equal to 0, then  $R$  is parallel to  $P$ . If this is the case and the volume of the tetrahedron defined by its vertices  $(L_0, a_0, b_0)$ ,  $(L_1, a_1, b_1)$ ,  $(L_2, a_2, b_2)$ , and  $(L_3, a_3, b_3)$  is greater than 0, then the intersection of  $R$  and  $P$  is empty. If  $R$  is parallel to  $P$  and the volume of the tetrahedron is equal to 0, then we should solve a ray tracing subproblem on the plane  $P$ , which turned out to contain  $R$ . Let  $R'$  be the ray emanating from  $(L_0, a_0, b_0)$  and passing through  $(L, a, b)$ . We find all points of intersection of  $R'$  with the sides of the triangle defined by

$(L_1, a_1, b_1)$ ,  $(L_2, a_2, b_2)$ , and  $(L_3, a_3, b_3)$ . If any such points exist, we locate among them the closest one to  $(L_0, a_0, b_0)$  and the farthest one from  $(L_0, a_0, b_0)$ . Finally, if R is not parallel to P, then the intersection of R and P is a single point  $(L', a', b')$ , and this case is illustrated in Fig. 1. Let's define

$$\mathbf{u} = [L_1 - L_0 \ a_1 - a_0 \ b_1 - b_0]^T \quad (5)$$

and compute

$$t = \langle \mathbf{n}, \mathbf{u} \rangle / \langle \mathbf{n}, \mathbf{v} \rangle. \quad (6)$$

Then

$$L' = L_0 + t(L - L_0), \quad (7)$$

$$a' = a_0 + t(a - a_0), \quad (8)$$

$$b' = b_0 + t(b - b_0). \quad (9)$$

Now let's check if the intersection point is inside the triangle. Let

$$\mathbf{x}' = [L' \ a' \ b']^T, \quad (10)$$

$$\mathbf{n}_{12} = (\mathbf{x}_2 - \mathbf{x}_1) \times (\mathbf{x}' - \mathbf{x}_1), \quad (11)$$

$$\mathbf{n}_{23} = (\mathbf{x}_3 - \mathbf{x}_2) \times (\mathbf{x}' - \mathbf{x}_2), \quad (12)$$

$$\mathbf{n}_{31} = (\mathbf{x}_1 - \mathbf{x}_3) \times (\mathbf{x}' - \mathbf{x}_1). \quad (13)$$

The intersection point  $(L', a', b')$  is inside the triangle defined by its vertices  $(L_1, a_1, b_1)$ ,  $(L_2, a_2, b_2)$ , and  $(L_3, a_3, b_3)$  if and only if  $\langle \mathbf{n}, \mathbf{n}_{12} \rangle \geq 0$ ,  $\langle \mathbf{n}, \mathbf{n}_{23} \rangle \geq 0$ , and  $\langle \mathbf{n}, \mathbf{n}_{31} \rangle \geq 0$ . If  $t \geq 0$ , then  $(L', a', b')$  is also the point of intersection of the triangle and the ray  $R'$ .

We set  $L_0=L$ ,  $a_0=0$ , and  $b_0=0$  and observe that  $(L_0, a_0, b_0)$  is now guaranteed not to coincide with  $(L, a, b)$ . Furthermore, by inspecting the distances between  $(L_0, a_0, b_0)$  and the intersection points found for the convex hull triangles, we can determine the maximum achievable chroma for our  $(L, h)$ -pair. We will denote this value as

$$C_{\max}(L, h) = \sqrt{a_{\max}^2 + b_{\max}^2}, \quad (14)$$

where  $(L, a_{\max}, b_{\max})$  is the farthest from  $(L_0, a_0, b_0)$  point of intersection of  $R'$  and a convex hull triangle. Similarly, we can compute

$$C_{\min}(L, h) = \sqrt{a_{\min}^2 + b_{\min}^2}, \quad (15)$$

where  $(L, a_{\min}, b_{\min})$  is the closest to  $(L_0, a_0, b_0)$  point of intersection of  $R'$  and a convex hull triangle.

Whenever at least one intersection point is found for a given  $(L, h)$ -pair, we add  $(a_{\max}, b_{\max})$  to the (initially empty) set of points that form the boundary of the color gamut slice at L. Moreover, if at least one intersection point is found for  $(L, h)$ , but no intersection points exist for  $(L, h+180^\circ)$ , then  $(a_{\min}, b_{\min})$  is also added to the set of the slice boundary points. This is needed, because the point

$(L_0, a_0, b_0) = (L, 0, 0)$  is not guaranteed to be inside the gamut even if L is achievable. In particular, the "white" and "black" points of a realistic color gamut routinely deviate from the L axis in CIELAB. We assume that  $R'$  exits the gamut no more than once.

Figure 2 shows the color gamut slices at  $L=50$  computed from the measurement data for the SWOP standard<sup>9</sup> using three methods: convex hull, "concave" hull, and ray tracing. The CIELAB data is known for 928 color patches of the standard IT8.7/3 target.

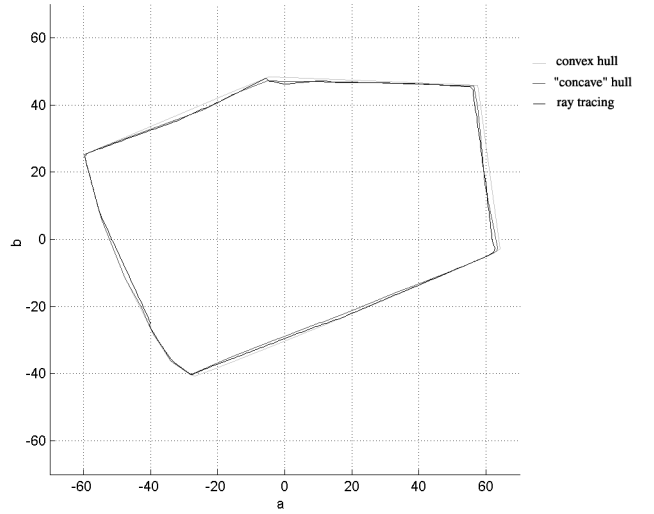


Figure 2. SWOP color gamut slices at  $L=50$

Let  $\Delta L$  and  $\Delta h$  be the distances between the adjacent sampling points. In our example,  $\Delta L=1$  and  $\Delta h=1^\circ$ . Let  $C_{\min}^2(L, h) = C_{\min}^2(L, h)$  if  $(a_{\min}, b_{\min})$  is a slice boundary point,  $C_{\min}^2(L, h) = 0$  otherwise. Set the value of  $C_{\max}^2(L, h)$  to 0 whenever  $R'$  does not intersect any of the convex hull triangles. Then the CIELAB volume of the color gamut can be approximated by the formula

$$V = \sum_{L, h} \left( \frac{\Delta L \cdot \pi \cdot \Delta h}{360^\circ} \left\{ C_{\max}^2(L, h) - C_{\min}^2(L, h) \right\} \right). \quad (16)$$

Precision of this approximation will improve as the device space is sampled sufficiently uniformly in more locations,  $\Delta L \rightarrow 0$ ,  $\Delta h \rightarrow 0$ , and the measurement equipment gets better. It will then be limited by the device's own variability. Table 1 provides the results of comparison of the values of several color gamut characteristics (including the CIELAB volumes) computed using three methods: convex hull, "concave" hull, and ray tracing. The CIELAB data for a set of 1012 coated PANTONE colors came from Ref. [10]. As you can see from the table, the conventional convex hull method overestimates the CIELAB volume of the SWOP color gamut by approximately 7%. If the number of  $(L, h)$ -pairs is doubled so that  $\Delta L=0.5$ , then the

gamut volume computed via ray tracing becomes 307,197 (instead of 307,195). I conducted an additional experiment on an electrophotographic imaging device with the gamut size considerably larger than that of SWOP. Having measured the same print of the 928-patch IT8.7/3 target twice on the same day with the same GretagMacbeth SpectroScan spectrophotometer unit, I determined that the measurement-to-measurement volume difference was between 0.01% and 0.03% of the smaller of the two volumes involved in its computation for the three methods of interest. In the meanwhile, the reduction of  $\Delta L$  from 1 to 0.5 produced the volume difference for the ray tracing method within 0.012% of the smaller volume. This result suggests that the precision of the ray tracing method with respect to the gamut volume is comparable to the precision of measurement. The same print was immediately measured with another SpectroScan unit, and the resulting instrument-to-instrument volume differences turned out to be within 0.18% for the three methods. The volume difference between ray tracing and the “concave” hull method remained within 0.6%, and the convex hull method continued to overestimate the gamut volume by approximately 7%.

**Table 1. Comparison of Color Gamut Characteristics**

L	PANTONE	SWOP		
	convex hull	“concave” hull	ray tracing	
<i>CIELAB volumes</i>				
	1,082,301	329,304	305,367	307,195
<i>Percentage of PANTONE colors inside gamut</i>				
	100%	31.9%	30.1%	29.5%
<i>Areas of gamut slices at L=10,20,...,90</i>				
10	1,669	121	119	115
20	6,260	1,753	1,745	1,613
30	10,743	4,115	4,046	3,926
40	15,238	6,260	6,072	6,016
50	18,494	7,693	7,460	7,443
60	19,290	6,599	6,054	6,192
70	17,350	4,441	3,614	3,898
80	12,990	1,901	1,419	1,465
90	6,482	0	0	0
<i>The totals of the gamut slice areas above</i>				
	108,514	32,883	30,528	30,669

### 3. Application to Device Profile Generation

For the purpose of the device profile generation, the set of (L,h)-pairs for ray tracing is derived from the set of grid points in the PCS (profile connection space) that have to be mapped to the device space. This derivation is likely to involve lightness compression (uniform or non-uniform), as most gamut mapping algorithms start with it.<sup>11,12</sup> The ray

tracing method allows to determine which of the (L,h)-pairs correspond to the CIELAB points outside the gamut. Morovic<sup>11</sup> lists a significant number of color mapping studies where clipping is given preference over compression. Once a line along which the rest of the mapping is to be carried out is determined, ray tracing along that line offers a way to implement clipping. Indeed, knowing the closest to (L,a,b) intersection point of the line of mapping and a convex hull triangle, it is straightforward to approximate the device space solution by means of interpolation, as the device space coordinates of the vertices of the closest triangle are known. Mapping of the interior points for the cases of CMY and CMYK printing can be performed as described by Hardeberg and Schmitt.<sup>13</sup>

### 4. Conclusions

A new method for color gamut characterization was introduced. It characterizes the gamut surface and volume more precisely than the conventional technique based on computing the convex hull of all measurement data points in CIELAB. The new approach involving ray tracing on the set of “local” convex hulls is useful for generation of device profiles.

### 5. Acknowledgments

The author thanks Eric K. Zeise, Chunghui Kuo, Yee Ng, H. T. Tai, and Jeffrey Wang of NexPress Solutions LLC for their help and advice.

### References

1. Specification ICC.1:2001-12, File Format for Color Profiles, ICC (2002), <http://www.color.org>.
2. T. J. Cholewo and S. Love, Gamut Boundary Determination Using Alpha-Shapes, Proc. of the 7<sup>th</sup> Color Imaging Conference: Color Science, Systems, and Applications, Scottsdale, AZ (1999) pp. 200-204.
3. R. W. G. Hunt, Measuring Colour, Fountain Press, Kingston-upon-Thames, England, third edition (1998).
4. K. Guyler, Visualization of Expanded Printing Gamuts Using 3-Dimensional Convex Hulls, TAGA (2000).
5. C. B. Barber, D. P. Dobkin, and H. Huhdanpaa, The Quickhull Algorithm for Convex Hulls, ACM Trans. on Mathematical Software, 22, 4 (1996) pp. 469-483.
6. R. Balasubramanian and E. Dalal, A Method for Quantifying the Color Gamut of an Output Device, Proc. of SPIE, 3018 (1997) pp. 110-116.
7. G. J. Braun and M. D. Fairchild, Techniques for Gamut Surface Definition and Visualization, Proc. of the 5<sup>th</sup> Color Imaging Conference: Color Science, Systems, and Applications, Scottsdale, AZ (1997) pp. 147-152.
8. R. J. Rolleston, Visualization of Colorimetric Calibration, Proc. of SPIE, 1912 (1993), pp. 299-309.
9. A. Taggi, D. McDowell, Graphic Technology—Color Characterization Data for Type 1 Printing, ANSI CGATS TR 001-1995, ANSI (1995).

10. PANTONE ColorDrive ® Professional, Pantone, Inc. (1996).
11. J. Morovic, Gamut Mapping and ICC Rendering Intents, Proc. of International Colour Management Forum, Derby, England (1999).
12. C. Cui, Gamut Mapping with Enhanced Chromaticness, Proc. of the 9<sup>th</sup> Color Imaging Conference: Color Science and Engineering, Scottsdale, AZ (2001), pp. 257-261.
13. J. Y. Hardeberg and F. Schmitt, Color Printer Characterization Using a Computational Geometry Approach, Proc. of the 5<sup>th</sup> Color Imaging Conference: Color Science, Systems, and Applications, Scottsdale, AZ (1997) pp. 96-99.

## **Biography**

**Dmitri A. Gusev** received an Honours Diploma in applied mathematics from Moscow Institute of Radioengineering, Electronics, and Automation in 1993, and M.S. and Ph.D. degrees in computer science from Indiana University in 1996 and 1999, respectively. He has been with NexPress Solutions LLC since 1999, where he is currently an image processing scientist. His research interests include color reproduction, digital halftoning, image compression, and image quality metrics. He is a member of the IS&T.